Published online 18 January 2008 *Nucleic Acids Research, 2008, Vol. 36, No. 5* ***1443–1449***
doi:10.1093/nar/gkm1146

Interaction of cationic surfactants with DNA: a single-molecule study

Sudhir Husale[1], Wilfried Grange[2,*], Marc Karle[3], Stephan Bürgi[4] and Martin Hegner[2]

[1]Rowland Institute at Harvard, Harvard University, 100 Edwin H Land Blvd., Cambridge MA 02142, USA, [2]Centre for Research on Adaptive Nanostructures and Nanodevices, Trinity College Dublin, College Green, Dublin 2, Ireland, [3]HSG-IMIT—Institute for Micromachining and Information Technology, Wilhelm-Schickard-Strasse 10, 78052 Villingen-Schwenningen, Germany and [4]Department of Chemistry, University of Basel, St. Johanns–Ring 19, CH-4056 Basel, Switzerland

Received October 22, 2007; Revised December 3, 2007; Accepted December 10, 2007

ABSTRACT

The interaction of cationic surfactants with single dsDNA molecules has been studied using force-measuring optical tweezers. For hydrophobic chains of length 12 and greater, pulling experiments show characteristic features (e.g. hysteresis between the pulling and relaxation curves, force-plateau along the force curves), typical of a condensed phase (compaction of a long DNA into a micron-sized particle). Depending on the length of the hydrophobic chain of the surfactant, we observe different mechanical behaviours of the complex (DNA-surfactants), which provide evidence for different binding modes. Taken together, our measurements suggest that short-chain surfactants, which do not induce any condensation, could lie down on the DNA surface and directly interact with the DNA grooves through hydrophobic–hydrophobic interactions. In contrast, long-chain surfactants could have their aliphatic tails pointing away from the DNA surface, which could promote inter-molecular interactions between hydrophobic chains and subsequently favour DNA condensation.

INTRODUCTION

DNA condensation is a fundamental process that has implications in both applied [e.g. gene delivery (1,2)] and basic research (3). Condensation of DNA can be achieved using either cations of charge +3 or greater (that neutralize 90% of the charge of DNA) or poor solvents (that make interactions of DNA with its environment less favourable) (4). As for multivalent cations (having a valence $\geq$3), monovalent cationic surfactants with sufficient long hydrophobic chains have the capability to condense large DNA molecules into micron-sized particles (4,5).

Still, the interaction of DNA with surfactants is of debate. In a recent study, Zhu and Evans (6) have suggested that the binding of surfactants with DNA proceeds through the formation of surfactant aggregates on the DNA [forming in solution and the presence of polymer chains (e.g. DNA) when the surfactant concentration is above the critical aggregate concentration (CAC)] that subsequently associate with the phosphate groups of DNA. This result differs from previous studies (both experimental and theoretical), which have proposed that a single surfactant monomer could interact with DNA solely through charge–charge interactions and subsequently catalyse the binding of additional molecules (7,8).

Various experimental methods have been used in the past to study the interaction of DNA and surfactants: surface tension, fluorescence, isothermal titration calorimetry, UV spectroscopy (3). Using these methods, ensemble properties can be determined (e.g. thermodynamics) from which the local binding mode of these surfactants with DNA may be indirectly determined. Direct and probably more precise information can also be obtained from ultra-sensitive techniques [atomic force microscopy, optical or magnetic tweezers (9–11)] that probe the intra- and inter-molecular forces of single molecules (e.g. DNA). For instance, the persistence length (the stiffness of a polymer chain) and the stretch modulus

*To whom correspondence should be addressed. Tel: +353 1 896 4502; Fax: +353 1 896 3037; Email: wilfried.grange@tcd.ie
Correspondence may also be addressed to Martin Hegner. Tel: +353 1 896 2285; Fax: +353 1 896 3037; Email: martin.hegner@tcd.ie
Former address:
Sudhir Husale, Wilfried Grange, Marc Karle and Martin Hegner, NCCR Nanoscale Science, Institute of Physics, University of Basel, Klingelbergstrasse 82, CH-4056 Basel, Switzerland.

The authors wish it to be known that, in their opinion, the first two authors should be regarded as joint First Authors.

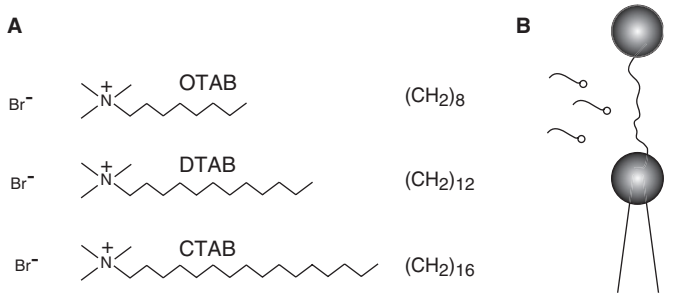

Figure 1. (**A**) The chemical structure of the surfactants studied in this work. (**B**) Schematic of an optical tweezers experiment. A single dsDNA molecule is tethered between two micron-sized polystyrene beads. One of these beads is placed on a micropipette (that can be moved with nanometer accuracy), while the second is trapped with two counter-propagating laser beams and acts as a very precise force-sensor (sub -pN accuracy). Experiments are performed in buffer conditions and at room temperature.

(the resistance to longitudinal strain) of DNA are relevant physical parameters (directly accessible from pulling experiments), which are sensitive to slight deformations in the DNA structure (12) and in turn reveal different interaction modes of bound molecules (e.g. surfactants) to DNA.

Here, we report on optical tweezers experiments performed in different modes of operation (pulling, force-clamp) on single double-stranded DNA (dsDNA) molecules in the presence of various cationic surfactants [octyl-trimethyl-ammonium bromide (OTAB), dodecyl-trimethyl-ammonium bromide (DTAB) and cetyl-trimethyl-ammonium bromide (CTAB), Figure 1A]. For aliphatic chains of length 12 and greater (DTAB, CTAB), a compaction of the DNA is observed at concentrations much lower than the critical micelle concentration (CMC, i.e. the concentration at which surfactant molecules form disperse aggregates in the absence of polymer chains). While DTAB– and CTAB–DNA complexes display a stretch modulus and a persistence length comparable to that of bare dsDNA, OTAB–DNA complexes (aliphatic chain length of 8) show a different mechanical response. From these observations, we suggest that short chain lengths surfactant molecules (OTAB) can lie down on the DNA surface, while longer chains (DTAB, CTAB) do not, enabling inter-molecular interactions between different chains and subsequent condensation.

MATERIALS AND METHODS

Surfactants

OTAB, DTAB and CTAB were purchased from Sigma (Basel, Switzerland). The CMC of the compounds are found to be 140 mM, 12 mM and 1 mM for OTAB, DTAB and CTAB, respectively (13). Both the CAC and CMC can be directly obtained from surface-tension measurements. Note that the CAC/CMC ratio is lower than unity and is for example of about 0.01 for CTAB (14,15).

DNA preparation

DNA molecules were prepared by PCR amplification [*Taq* DNA Polymerase (Roche, Basel, Switzerland)] of the pTYB1 plasmid (7477 bp) (New England Biolabs, Ipswich, MA) using 5′-Thiol-TGT AAC TCG CCT TGA TCG TTG GGA-3′ and 5′-AGC GGA TAC ACC AGG ATT TGT CGT-3′ as forward and reverse primers (Microsynth, Basel, Switzerland), respectively. The 6587-bp PCR fragment was digested with HindIII (NEB). Finally, the main fragment was end-filled with Klenow Exo- (NEB) with dGTP and biotin-14-dUTP, dATP, dCTP (Invitrogen, Basel, Switzerland), yielding a 5623-bp long dsDNA. Subsequently, DNA molecules were covalently coupled to 2.17-micron amino-modified beads (Spherotech, Libertyville, IL) using a procedure similar to that of Ref. (16).

Optical tweezers

The experimental apparatus for the optical tweezers experiments has been described (17). DNA-beads were trapped by the laser and the free biotinylated DNA end was attached to a 2.20-micron streptavidin bead (Spherotech), which was held by suction on a micropipette (Figure 1B). The bead-to-bead distance was determined from both the movement of the micropipette (controlled with a closed-loop piezoelectric element) and the deflection of the laser producing the optical trap (monitored by a 2D position sensitive detector). 150 mM NaCl, 10 mM HEPES pH 7.5, 1 mM EDTA and 1 mM NaN_3 was used as a standard buffer throughout all experiments. Cationic surfactants were injected at an average flow speed of ~25 µl/min by gravity flow (the buffer containing the surfactants is stored in a reservoir connected to the fluid chamber and the flow speed is controlled by adjusting the height of the syringe with respect to the outlet of the chamber). Force versus extension curves were recorded at zero flow, while force-clamp measurements were recorded in a constant-flow mode (for this mode of operation, the direction of the applied force was perpendicular to that of the flow). Typical force curves were measured at a constant velocity of 150 and 450 nm/s, respectively. For this mode of operation, both the stretching and relaxing of the molecule under study were recorded. For both force- and distance-clamp experiments, data were acquired at a rate of 50 Hz. At each surfactant concentration, experiments were performed on about 10 different molecules for which multiple traces were recorded. Unless specified in the text, force curves shown in this study represent a stable configuration at full coverage.

RESULTS AND DISCUSSION

Mechanics of bare dsDNA

Figure 2 shows a typical force versus extension curve of bare DNA measured in assembly buffer (grey circles). For forces below ~60 pN, the mechanical response $F(x)$ of a DNA molecule (with persistence length P, stretch modulus

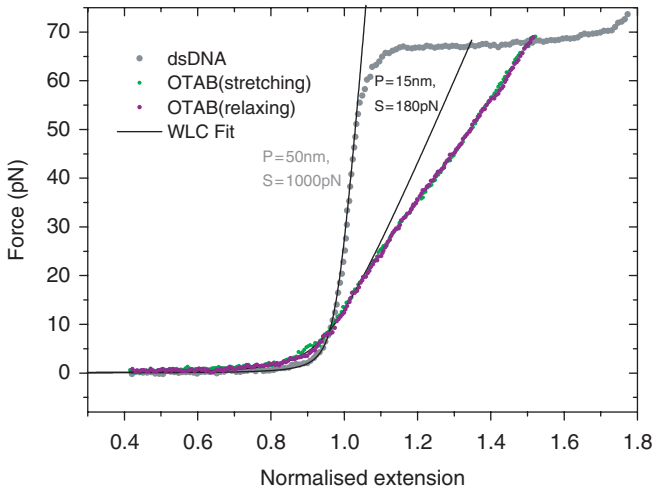

Figure 2. Typical force versus extension curves obtained for bare dsDNA (grey circles), dsDNA in the presence of OTAB (green and purple circles, showing the stretching and relaxing part of the curve). Force curves were recorded in assembly buffer (150 mM NaCl, 10 mM HEPES pH 7.5, 1 mM EDTA, 1 mM NaN_3) in a constant flow mode (pulling speed: 450 nm/s). [OTAB] = 80 mM. Force curves are normalized to the contour length L_0 of dsDNA (1911 nm). Also shown are WLC fits (black line) to the experimental traces [P denotes the persistence length, S is the stretch modulus, see Equation (1)]. Experiments performed on ~10 molecules in the presence of OTAB yield P and S values of (180 ± 30) pN and (15 ± 4) nm, respectively.

S and contour length L_0) follows an extended worm-like-chain extension (WLC) (18,19):

$$\frac{FP}{k_B T} = \frac{1}{4}\left[1 - \frac{x}{L_0} + \frac{F}{S}\right]^{-2} - \frac{1}{4} + \frac{x}{L_0} - \frac{F}{S} \qquad \mathbf{1}$$

where $k_B T = 4.1$ pN·nm at room temperature.

Using standard buffer conditions (150 mM NaCl, pH ~ 7.5), DNA molecules show a stretch modulus of ~1000 pN and a persistence length of ~50 nm, respectively. At ~65 pN an overstretching of DNA is observed, yielding a 70% increase of the contour length for a small range of applied forces ~2 pN (13). The existence of this overstretching plateau has led to many theoretical discussions and its origin is still of debate (20).

Force versus extension curves in the presence of surfactants

To investigate the elastic response of DNA interacting with cationic surfactants, bare dsDNA molecules were kept stretched at ~80% of their contour length while injecting the surfactant molecules. Subsequently, force-extension curves were recorded. The results presented in this section were found to be highly reproducible (Supplementary Data).

Figure 2 shows that the binding of short single-chain OTAB molecules [aliphatic chain length of $(CH_2)_8$, 80 mM] affects the mechanical properties of the DNA (grey circles—bare dsDNA) (pulling speed: 450 nm/s). Note that the stretching and relaxing parts of the force curves (green and purple circles, respectively) superimpose. This demonstrates that force curves are completely reversible for the range of speeds used in the experiment (from 150 to 450 nm/s) (Figure S1, showing experiments performed at various speeds and on different DNA molecules). A fit using Equation (1) yields a persistence length of (15 ± 4) nm and a stretch modulus of (180 ± 30) pN, respectively (black line). At high forces ($F \geq 40$ pN), force curves show a change in the elasticity of the stretched molecule. This could be attributed to a change in the interaction between the surfactants and the DNA as the force is increased. A similar behaviour was observed for YOYO-1 and Ethidium Bromide (21).

As seen in Figure 3, force versus extension curves measured in the presence of DTAB [aliphatic chain length of $(CH_2)_{12}$] show at concentrations of 200 μM and above a force-plateau along the curve (up to 0.9 fractional extensions) (pulling speed: 150 nm/s). This plateau, centred at ~5–10 pN (Figure 3), which occurs at concentration much lower than the CMC of 12 mM, indicates that DNA compacts into a globular structure (19). Further evidence for DNA condensation is obtained from force-clamp experiments at 2.5 pN (i.e. the pipette displacement is controlled by a servo-system to maintain a constant tension on the DNA during surfactant injection), where we observe a rapid change in the DNA length (compaction) upon DTAB binding (Figure 4). Similar curves were also obtained from force-clamp measurements at forces below ~10 pN (data not shown).

CTAB [aliphatic chain length of $(CH_2)_{16}$] also forms a condense phase with DNA (Figure 3) (pulling speed: 150 nm/s). For some of the measured curves, a pronounced sawtooth-like extension pattern up to 0.9 fractional extensions is observed. A similar behaviour (rarely present for DTAB, Figure 3) was first observed when DNA was condensed by multivalent cations (19,22) and was attributed to the sudden unfolding (opening) of collapsed structures. Here, we observe that DNA condensation can occur at concentrations orders of magnitude smaller than the CMC (1 mM for CTAB). For instance, a deviation from the expected mechanical behaviour of bare dsDNA is found at a concentration of ~10 μM. This is in good agreement with both ensemble measurements as well as fluorescence microscopy investigations (from which the condensation of DNA into a globular structure is readily seen) (5). As seen in Figure 3, force curves show a pronounced hysteresis at low extensions. This hysteresis, also observed for DTAB, indicates that the system is not under full equilibrium even at a pulling speed of 150 nm/s (see below).

Interestingly, a small reduction in the contour length (up to 10%) is observed for both DTAB and CTAB. Such a reduction has also been reported for dendrimers (11) and probably indicates that some regions along the DNA remain condensed at high force. This is in agreement with the observation that subsequent pulls (at non-complete coverage) give rise to a slight shift in the fractional extension at which the force starts to raise (Figure S2, showing the progressive dissociation of surfactants).

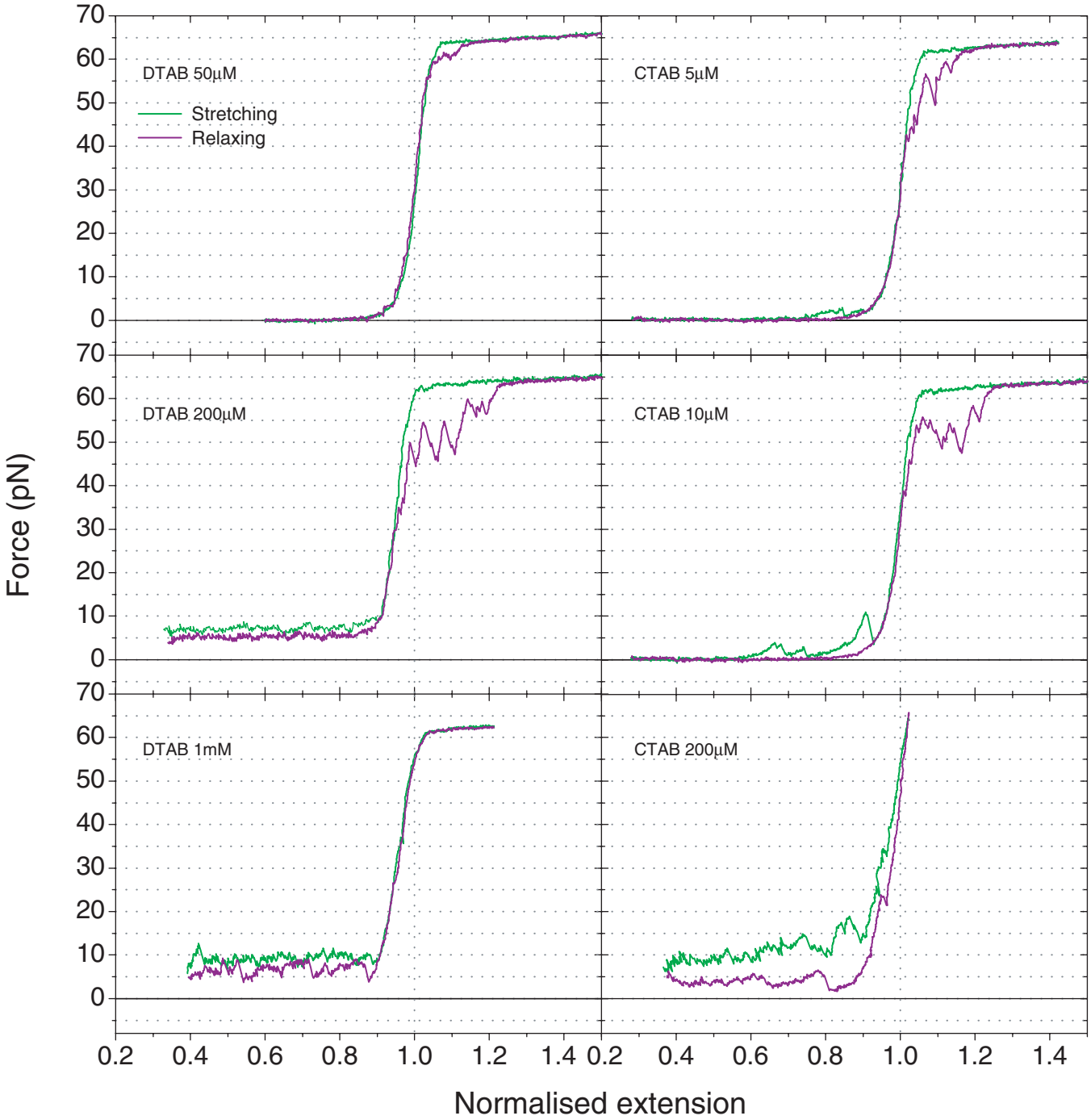

Figure 3. Typical force versus extension curves obtained for dsDNA in the presence of DTAB and CTAB. Force curves were recorded in assembly buffer and for different concentrations of the surfactant molecules. Pulling speed: 150 nm/s. The force versus extension curves are normalized to the contour length of dsDNA (1911 nm). Both the stretching and relaxing parts of the curves are highlighted (green and purple lines, respectively). For dsDNA and assuming a persistence length of 54 nm and a stretch modulus of 1000 pN, the WLC model predicts that the force reaches a value of ~26 pN at its contour length. The existence of a plateau along the pulling curve or sawtooth-like extension patterns evidences for the presence of a condensed phase (observed above 200 µM for DTAB and above 10 µM for CTAB).

Two-states model

We present here a simple theoretical model that reproduces typical features observed for force-extension curves in the presence of a condensed phase (DTAB, CTAB). The model is based on Bell's theory (refined by Evans) (23,24), which considers that the activation barrier for bond dissociation (having a width x) is reduced by Fx in the presence of a defined force F. Considering that the intermolecular contacts between different aliphatic chains consist of a two-level system that can undergo a transition

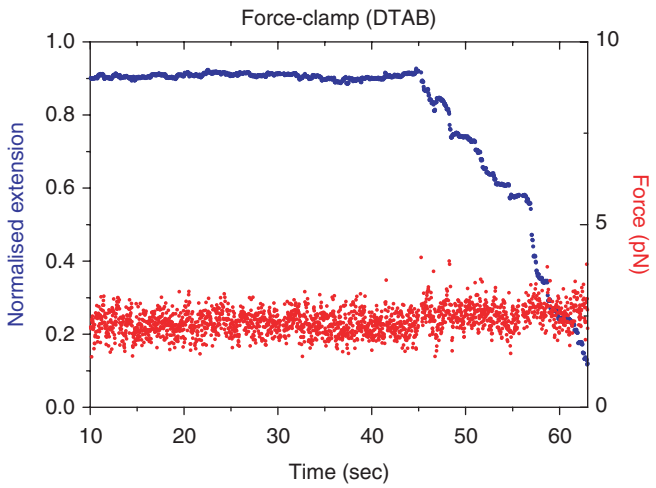

Figure 4. Force-clamp experiment (force set at 2.5 pN, red circles) showing the collapse of dsDNA (blue circles) upon DTAB interaction (at $\sim t = 45$ s). (DTAB) = 1 mM. The time it takes for the surfactant molecules to reach and interact with the tethered DNA is undefined as it depends on the volume of the optical tweezers chamber as well as the flow speed.

from a 'folded' to 'unfolding' configuration (and vice versa), we have:

$$\alpha(F) = \alpha_0 \exp(Fx_{\text{unfolding}}/\gamma) \quad \mathbf{2}$$

and

$$\beta(F) = \beta_0 \exp(-Fx_{\text{folding}}/\gamma) \quad \mathbf{3}$$

where

α (β) is the force-dependent rate for unfolding (folding), $\gamma = 4.11$ pN·nm at room temperature, x is the width of the activation barrier (considered to be asymmetric for unfolding and folding) and α_0 (β_0) is the rate at zero force. Following the method described in Ref. (25), we calculate the probability for any of the contacts (N_{bound}) in between two surfactant molecules bound to DNA to break (to unfold) during a time interval Δt (corresponding to a change Δx in the pipette position of the optical tweezers) (25):

$$P_{\text{unfolding}} = N_{\text{bound}}\alpha(F)\Delta t \quad \mathbf{4}$$

Similarly, the probability for folding is

$$P_{\text{folding}} = (N_0 - N_{\text{bound}})\beta(F)\Delta t \quad \mathbf{5}$$

where N_0 is the number of bound molecules at $t = 0$, i.e. $N_0 = N_{\text{bound}}$. At each time interval (each movement Δx), we estimate the force according to Equation (1) and allow the folding (unfolding) transition to occur (given rise to a change in extension of L_a) based on a random number decision.

The results of the simulations are shown in Figure 5 (black line) using a speed and a step size identical to that of the experiments (150 and 450 nm/s, respectively). Using two different pulling speeds for the simulation considerably reduces the choice of the fitting parameters. Simulated curves were found to reproduce qualitatively the data with $P = 54$ nm and $S = 1000$ pN (identical to that of bare dsDNA) and an energy barrier for the transition of $8.7\,k_BT$ ($5.3\,k_BT$) for CTAB (DTAB). Other parameters are given in Ref. (26).

Although the simulation only partially reproduces the detailed structure of the experimental force curves (e.g. observed reduction in contour length), it correctly predicts the main features: existence of a force-plateau (DTAB, CTAB) and strong hysteresis between the extension and relaxation curves (CTAB).

Dissociation of surfactants

By depleting the concentration of the surfactant molecules (i.e. by flushing the chamber with the assembly buffer, Figure S2), the DNA again adopted its natural B-form conformation (as shown by force versus extension curves). This reversibility (occurring in a monotonic manner) was rapidly observed for OTAB, CTAB and DTAB [i.e. after an ~5-min (125 µl) wash].

DISCUSSION

First, our results help to clarify some controversial results found in the literature. For instance, Figure 3 indicates that DTAB not only binds but also condenses dsDNA. This result strengthens the calorimetric ensemble experiments (Isothermal Titration Calorimetry) (8), which evidence for a condensation in contrast to other binding and thermodynamic studies (7).

Second, the measured condensation forces for DTAB and CTAB (magnitude of the condensing plateau) are found to be comparable to multivalent cations [CoHex (~4 pN) (19) and Spermidine (~1 pN) (22)] and polyaminoamide dendrimers (~10 pN) (11). The process of condensation is however different for cationic surfactants. For these compounds, condensation is strongly influenced by the fact that these cationic surfactants are directly linked to an aliphatic chain, which favours a minimization of the hydrophobic interfaces by collapsing into a compacted structure in an aqueous environment.

Third, force versus extension curves (and the mechanical parameters derived from such measurements) show different mechanical behaviours as the length of the hydrophobic tail is varied. We have found that OTAB [$(CH_2)_8$] does not condense DNA but strongly affects both the persistence length (P) and the stretch modulus (S) of dsDNA. Interestingly, CTAB and DTAB, which have a longer aliphatic carbon chain, do not noticeably alter the mechanical characteristics of dsDNA. Indeed, the simulations (Figure 5) reproduce nicely both the local curvature (e.g. the persistence length, as observed on the force curves at a normalized extension of ~0.9, see Figure 5) and the slope at high forces (stretch modulus) of the measured experimental force curves using P and S values typical of dsDNA.

These results provide an important insight on the interaction of surfactants with DNA. From our investigations, we conclude that the binding mode of OTAB is different than that of intercalators or major- (minor) groove binders (e.g. SYBR-Green I) for which an increase

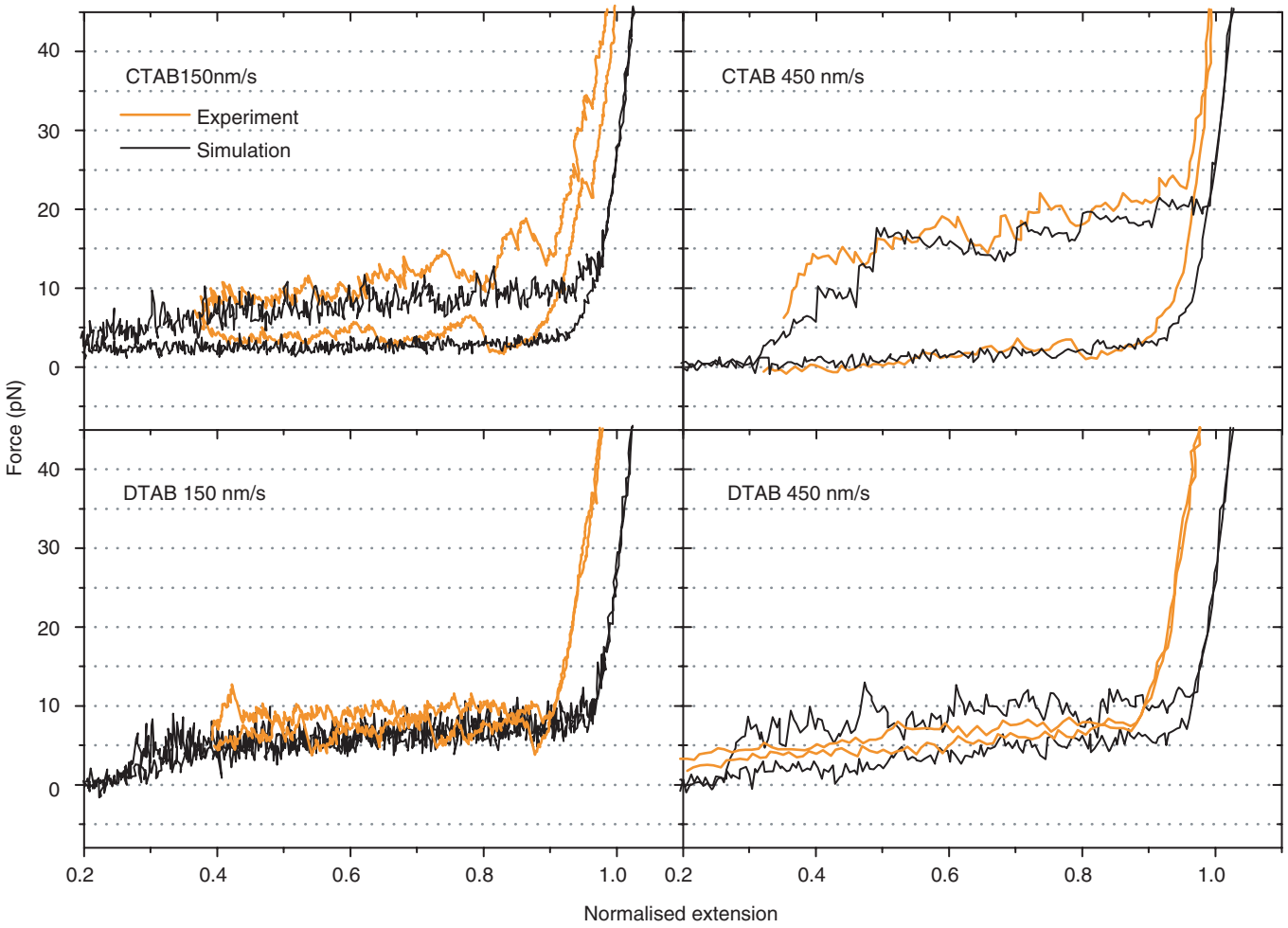

Figure 5. Simulations of the experimental traces of both DTAB and CTAB (black) obtained in a two-states model (see text) using values for the persistence length P and stretch modulus S identical to that of dsDNA. Simulations are performed for a pulling speed of 150 and 450 nm/s, respectively. The model reproduces specific features of the experiment: evidence of a defined force-plateau at a few pN (DTAB and CTAB) and a strong hysteresis for CTAB. Experimental curves measured for DTAB (CTAB) are also shown (orange). A noise of 0.5 pN and 2 nm has been added to the simulated traces to account for the experimental noise. (DTAB) = 1 mM, (CTAB) = 200 μM.

in contour length (intercalators) or a strong hysteresis of the force curves (minor- and major-groove binders) are observed (21,27). The interaction of these surfactants with DNA, although still unknown, could be due to hydrophobic–hydrophobic interactions of the DNA bases with the aliphatic surfactant tails. In other words, surfactants with short chain lengths could directly interact with the DNA bases surface, which, as a result, could strongly modify the stretch modulus. This binding mode is highly possible and has already been suggested by Matulis *et al.* (8) on the basis that short hydrophobic tails have sufficient space to lie down on the DNA. In contrast, we suggest that surfactants with longer hydrophobic chains [DTAB, CTAB, i.e. $(CH_2) \geq 12$] do not noticeably interact with the DNA surface. As for short-chain surfactants, the initial binding of DTAB and CTAB proceeds solely through electrostatic interactions (between the positive cations and the negatively charged DNA phosphates), but the interaction of the aliphatic tails with the DNA bases might be less favourable than a direct aliphatic contact between chains. This is evidenced by the fact that the stretch modulus (sensitive to slight deformation in the dsDNA structure) measured for both DTAB and CTAB remain almost similar to that of bare dsDNA. As a result, long chains most probably localize away from the DNA groove [which would otherwise lead to a change in the stretch modulus (12)] and reduce the contacts with the surrounding water by forming aggregates (promoting condensation).

Our single-molecule experiments also demonstrate that surfactant monomers are indeed able to bind and condense single dsDNA strands. This contrasts with recent ensemble experiments, which have shown that surfactant interactions are mediated by the interaction of surfactant aggregates with the negatively charged phosphate groups of DNA (6). Such aggregates are formed in the presence of oppositely charged polyelectrolytes (e.g. DNA) when the concentration of the surfactants is larger than the CAC (28). Although the concentration of the injected surfactants is quite high for some of our

experiments (half of the CMC), the surfactants remain in a pure monomeric state due to both the absence of other DNA molecules in the chamber and the speed of injection (~25 μl/min).

Finally, our measurements, in agreement with previous ensemble studies [e.g. for CTAB (5)], demonstrate that condensation can occur at concentrations much lower than the CMC (Figures 3 and 4).

CONCLUSION

We have used optical tweezers to investigate and clarify the interaction of some surfactants (OTAB, CTAB and DTAB) with dsDNA. For surfactants with sufficiently long hydrophobic chains (CTAB, DTAB), we have observed—in agreement with previous studies (8)—a transition from an extended to a condensed state (for which the DNA adopts a highly compacted structure). Depending on the chain length, pulling curves show different mechanical behaviours that directly correlate with the local binding mode of these surfactants on DNA. Short hydrophobic chain lengths (8) drastically modify the mechanical properties of DNA (persistence length, stretch modulus). In contrast, longer chains do not noticeably affect the DNA mechanics but do condense DNA. These observations suggest that short chain lengths can lie down on the DNA surface, while longer chains do not, allowing DNA condensation.

SUPPLEMENTARY DATA

Supplementary data are available at NAR Online.

ACKNOWLEDGEMENTS

Financial support is acknowledged from the Swiss National Foundation (SNF) (grants # 3152-67919.02, 3152A0-105953), the EUCOR Learning and Teaching Mobility (ELTEM) Nanotechnology project, the Endress Foundation, the National Center of Competence in Research 'Nanoscale Science' (NCCR) and the Centre for Research on Adaptive Nanostructures and Nanodevices (CRANN, SFI foundation). Funding to pay the Open Access publication charges for this article was provided by the Science Foundation Ireland.

Conflict of interest statement. None declared.

REFERENCES

1. Felgner,P.L., Gadek,T.R., Holm,M., Roman,R., Chan,H.W., Wenz,M., Northrop,J.P., Ringold,G.M. and Danielsen,M. (1987) Lipofection: a highly efficient, lipid-mediated DNA-transfection procedure. *Proc. Natl Acad. Sci. USA*, **84**, 7413–7417.
2. Storrie,H. and Mooney,D.J. (2006) Sustained delivery of plasmid DNA from polymeric scaffolds for tissue engineering. *Adv. Drug Deliv. Rev.*, **58**, 500–514.
3. Goddard,E.D. (2002) Polymer/surfactant interaction: interfacial aspects. *J. Colloid Interface Sci.*, **256**, 228–235.
4. Bloomfield,V.A. (1997) DNA condensation by multivalent cations. *Biopolymers*, **44**, 269–282.
5. Mel'nikov,S.M., Sergeyev,V.G. and Yoshikawa,K. (1995) Discrete coil-globule transition of large DNA induced by cationic surfactant. *J. Am. Chem. Soc.*, **117**, 2401–2408.
6. Zhu,D.-M. and Evans,R.K. (2006) Molecular mechanism and thermodynamics study of plasmid DNA and cationic surfactants interactions. *Langmuir*, **22**, 3735–3743.
7. Bathaie,S.Z., Moosavi-Movahedi,A.A. and Saboury,A.A. (1999) Energetic and binding properties of DNA upon interaction with dodecyl trimethylammonium bromide. *Nucleic Acids Res.*, **27**, 1001–1005.
8. Matulis,D., Rouzina,I. and Bloomfield,V.A. (2002) Thermodynamics of cationic lipid binding to DNA and DNA condensation: roles of electrostatics and hydrophobicity. *J. Am. Chem. Soc.*, **124**, 7331–7342.
9. Rief,M., Clausen-Schaumann,H. and Gaub,H.E. (1999) Sequence-dependent mechanics of single DNA molecules. *Nat. Struct. Biol.*, **6**, 346–349.
10. Bustamante,C., Bryant,Z. and Smith,S.B. (2003) Ten years of tension: single-molecule DNA mechanics. *Nature*, **421**, 423–427.
11. Ritort,F., Mihardja,S., Smith,S.B. and Bustamante,C. (2006) Condensation transition in DNA-polyaminoamide dendrimer fibers studied using optical tweezers. *Phys. Rev. Lett.*, **96**, 118301–118304.
12. Hegner,M., Smith,S.B. and Bustamante,C. (1999) Polymerization and mechanical properties of single RecA-DNA filaments. *Proc. Natl Acad. Sci. USA*, **96**, 10109–10114.
13. Lin,C.-E. (2004) Determination of critical micelle concentration of surfactants by capillary electrophoresis. *J. Chromatogr. A*, **1037**, 467–478.
14. Mel'nikov,S.M., Sergeyev,V.G. and Yoshikawa,K. (1995) Transition of double-stranded DNA chains between random coil and compact globule states induced by cooperative binding of cationic surfactant. *J. Am. Chem. Soc.*, **117**, 9951–9956.
15. Tam,K.C. and Wyn-Jones,E. (2006) Insights on polymer surfactant complex structures during the binding of surfactants to polymers as measured by equilibrium and structural techniques. *Chem. Soc. Rev.*, **35**, 693–709.
16. Hegner,M. (2000) DNA handles for single molecule experiments. *Singl. Mol.*, **1**, 139–144.
17. Grange,W., Husale,S., Guntherodt,H.J. and Hegner,M. (2002) Optical tweezers system measuring the change in light momentum flux. *Rev. Sci. Instrum.*, **73**, 2308–2316.
18. Bustamante,C., Marko,J.F., Siggia,E.D. and Smith,S. (1994) Entropic elasticity of lambda-phage DNA. *Science*, **265**, 1599–1600.
19. Baumann,C.G., Bloomfield,V.A., Smith,S.B., Bustamante,C., Wang,M.D. and Block,S.M. (2000) Stretching of single collapsed DNA molecules. *Biophys. J.*, **78**, 1965–1978.
20. Cocco,S., Yan,J., Leger,J.F., Chatenay,D. and Marko,J.F. (2004) Overstretching and force-driven strand separation of double-helix DNA. *Phys. Rev. E*, **70**, 11910–11918.
21. Sischka,A., Toensing,K., Eckel,R., Wilking,S.D., Sewald,N., Ros,R. and Anselmetti,D. (2005) Molecular mechanisms and kinetics between DNA and DNA binding ligands. *Biophys. J.*, **88**, 404–411.
22. Muruyama,Y., Sakamaki,Y. and Sano,M. (2003) Elastic response of single DNA molecules exhibits a reentrant collapsing transition. *Phys. Rev. Lett.*, **90**, 18102–18104.
23. Bell,G.I. (1978) Models for the specific adhesion of cells to cells. *Science*, **200**, 618–627.
24. Evans,E. and Ritchie,K. (1997) Dynamic strength of molecular adhesion bonds. *Biophys. J.*, **72**, 1541–1555.
25. Rief,M., Fernandez,J.M. and Gaub,H.E. (1998) Elastically coupled two-level systems as a model for biopolymer extensibility. *Phys. Rev. Lett.*, **81**, 4764–4767.
26. Simulation. CTAB. Contacts: 170, change in length (L_a): 10 nm, x_unfolding: 8 nm, x_folding: 0.8 nm. DTAB. Contacts:170, change in length (L_a): 10 nm, x_unfolding: 3 nm, x_folding: 0.5 nm.
27. Husale,S., Grange,W. and Hegner,M. (2002) DNA mechanics affected by small DNA interacting ligands. *Singl. Mol.*, **3**, 91–96.
28. Guillot,S., Delsanti,M., Desert,S. and Langevin,D. (2003) Surfactant-induced collapse of polymer chains and monodisperse growth of aggregates near the precipitation boundary in carboxymethyleellulose-DTAB aqueous solutions. *Langmuir*, **19**, 230–237.